universe MDPI

Review

Superfluid Phonons in Neutron Star Core

Marcello Baldo

INFN Sez. Catania, Via S. Sofia 64, 95126 Catania, Italy; baldol@ct.infn.it

Abstract: In neutron stars the nuclear asymmetric matter is expected to undergo phase transitions to a superfluid state. According to simple estimates, neutron matter in the inner crust and just below should be in the s-wave superfluid phase, corresponding to the neutron-neutron $^1S_0$ channel. At higher density in the core also the proton component should be superfluid, while in the inner core the neutron matter can be in the $^3P_2$ superfluid phase. Superluidity is believed to be at the basis of the glitches phenomenon and to play a decisive influence on many processes like transport, neutrino emission and cooling, and so on. One of the peculiarity of the superfluid phase is the presence of characteristic collective excitation, the so called 'phonons', that correspond to smooth modulations of the order parameter and display a linear spectrum at low enough momentum. This paper is a brief review of the different phonons that can appear in Neutron Star superfuid matter and their role in several dynamical processes. Particular emphasis is put on the spectral functions of the different components, that is neutron, protons and electrons, which reveal their mutual influence. The open problems are discussed and indications on the work that remain to be done are given.

Keywords: neutron stars; superfluidity; phonons

check for updates

Citation: Baldo, M. Superfluid Phonons in Neutron Star Core. *Universe* **2021**, 7, 16. https://doi.org/10.3390/universe7010016

Received: 18 November 2020
Accepted: 4 January 2021
Published: 14 January 2021

Publisher's Note: MDPI stays neutral with regard to jurisdictional claims in published maps and institutional affiliations.

1. Introduction

The microscopic excitations of nuclear matter are essential for an accurate description of the phenomena that occur in neutron stars and affect directly their properties, like transport processes or neutrino dynamics. They can be relevant also for neutrino emission and specific heath, which are all involved in the short and long time cooling evolution of the star. The elementary excitations of the superfluid matter are of special importance. In fact superfluidity is expected to be present in neutron star matter, and both the proton and the neutron components can be affected by the pairing phenomenon. Unfortunately the density dependence of both types of superfluidity is only roughly known, but their study can be of great help to untangle the interpretation of the observational data. For a recent review see ref. [1]. The fact that at not too high density the main components of the matter should be neutrons, protons, electrons and muons [2], implies that the general features and the spectral properties of these excitations can be quite complex. In the astrophysical physical conditions, a study of the collective microscopic excitations in normal neutron star matter has been presented in Ref. [3] within the relativistic mean field approximation. In refs. [4,5] the spectral functions of the neutron, proton and electron components of normal neutron star matter have been calculated microscopically within the non-relativistic Random Phase Approximation (RPA) for the nucleons and the relativistic RPA for the leptonic components. In this study different schemes for the nuclear effective interaction were adopted. In particular, a comparison was performed between a set of Skyrme forces and a microscopically derived interaction. In this context recently the relativistic RPA has been used also for the nucleon sector [6]. The study of refs. [4,5] were extended to include superfluid proton matter in ref. [7]. For simplicity the coupling of the superfluid protons with neutrons was neglected. The elementary excitations in superfluid neutron star matter have been considered by several authors [8–13]. In ref. [7] it was demonstrated that, due to the screening by electrons of the proton-proton Coulomb interaction, the proton superfluid matter, as demanded by a general theorem for short range interactions, possesses a pseudo-Goldstone mode below the pair breaking mode. According to [8–14] the presence of such excitation can have a strong effect on e.g. neutrino mean free path and their emission rate. As shown in ref. [15], the suerfluid phonons can be the trigger for vortex unpinning avalanches responsible of glitches formation. An extensive study of the elementary excitations in presence of both proton and neutron superfluidity has been presented in ref. [16], where the hydrodynamic formalism was used with the inclusion of proton-neutron coupling. In refs. [17,18] a study was presented of the elementary excitations in superfluid neutron matter in the crust. The possible presence of coupling with the nuclear lattice was considered in refs. [18–21] .

In this paper we presents a review on the theory and applications of the superfluid phonons in the astrophysical context of neutron stars. The paper is organized as follows. After the present introduction, the hydrodynamic treatment of the phonon excitations in superfluids is reported, which is based on the Landau theory of Fermi liquid. Next we consider the microscopic treatment based on the Green' s function formalism and the RPA approximation. Within the microscopic theory one can consider also phonon momenta that are not necessarily vanishing small, provided that they are still lower than the Fermi momentum. The role of the phonon degrees of freedom in different phenomena and in the properties of neutron stars are then reported from the existing literature. The final remarks are in the last section.

2. Theory of the Superfluid Phonons

2.1. Hydrodynamic Approach

Both boson superfluidity, e.g. in ^{4}He liquid, and superfluidity or superconductivity in Fermi systems can be described macroscopically by introducing the condensate field $\psi(\mathbf{r}, t)$ which has a smooth variation on position $\mathbf{r}$ and time t. In the ground state of a homogeneous system the field is uniform in space and it coincides with the order parameter of the condensate. Actually the phase of the field must have a linear dependence on time, as it can be shown from the microscopic theory, but this will not play a role in the following. The field can be excited and then it varies in space and time. According to Goldstone theorem [22,23], the symmetric (condensate) phase must possesses collective modes with a frequency that vanishes at zero momentum. These are the superfluid phonons in our case. The only exception is when the Coulomb interaction is present, because for long range forces the Goldstone theorem is invalid. Apart this case, that will be discussed later, we can then restrict the analysis in the long wavelength limit. For a macroscopic description it is convenient to introduce the current that represent the superfluid matter flow. In quantum mechanics the local current is given by

$$\mathbf{j} \,=\, -\frac{\imath\hbar}{2m}(\psi^*\nabla\psi \,-\, \psi\nabla\psi^*) \tag{1}$$

where in this case the condensate field is treated as a wave function. This can be justified if one interprets the field as the common wave functions of the physical objects that condensate, i.e., boson particles or Cooper pairs, with mass m. In the latter case it is just the pairing field, that is the wave function of the center of mass of the Cooper pair. Accordingly, for the total current we have to multiply by the total number of constituent particles. Since this factor can be finally dropped out from the formulae, we do not include it. Accordingly the local number density is given by

$$\rho(\mathbf{r}, t) \,=\, |\psi(\mathbf{r}, t)|^2 \tag{2}$$

We now separate modulus and phase of the field

$$\psi(\mathbf{r}, t) \,=\, \sqrt{\rho}\exp(\imath S) \tag{3}$$

If we now substitute (3) in (1), one gets

$$\mathbf{j}(\mathbf{r},t) \;=\; \frac{i\hbar}{m}\rho(\mathbf{r},t)\nabla S(\mathbf{r},t) \tag{4}$$

which shows that $\frac{i\hbar}{m}\nabla S(\mathbf{r},t)$ can be interpreted as the velocity field $\mathbf{v}$ at a given point. It has to pointed out that we are consider one component superfluid. If both neutrons and protons are superfluid, one has to consider entrainment and the relations between velocities and currents has to be modified [24]. Density and current satisfy the continuity equation

$$\frac{\partial\rho}{\partial t} \;+\; \nabla\mathbf{j} \;=\; 0 \tag{5}$$

which is a constraint that the dynamical evolution of the superfluid must satisfy.

Because the superfluid flow is without friction, the evolution of the velocity field can be described by the Euler equation for a perfect fluid

$$\frac{\partial}{\partial t}\,\mathbf{v} \,+\, \mathbf{v}\,\nabla\,\mathbf{v} \,+\, \nabla\mu(\mathbf{r},t) \;=\; 0 \tag{6}$$

where $\mu(\mathbf{r},t)$ is the local chemical potential. Equations (5) and (6) are the basic equations to be solved in this particular simple case. Because we are looking for small amplitude and long wavelength excitations, we can linearize the equations, that is we put

$$S(\mathbf{r},t) \;=\; S_0(t) \,+\, \phi(\mathbf{r},t) \qquad\qquad \rho(\mathbf{r},t) \;=\; \rho_0 \,+\, \delta\rho(\mathbf{r},t) \tag{7}$$

where ρ_0 is the ground state density and S_0 the ground state phase, which is $-\mu_0 t$, with μ_0 the ground state chemical potential. Then the equations are linearized with respect to ϕ and $\delta\rho$. Accordingly, due to the relation of $\mathbf{v}$ with S, in the Euler equation we can neglect the term quadratic in velocity and one gets

$$\nabla\,(\frac{\partial}{\partial t}S(\mathbf{r},t) \,+\, \mu(\mathbf{r},t)) \;=\; 0 \tag{8}$$

which indicates that the expression in parenthesis must be a constant independent of coordinates. The constant turns out to be zero, as can be deduced by the microscopic theory. This can be also guessed by noticing that it appears as a modification of the chemical potential by the same amount throughout the system, which would imply a macroscopic energy change at any given time. One then can write

$$\frac{\partial}{\partial t}S(\mathbf{r},t) \;=\; -\mu(\mathbf{r},t) \tag{9}$$

This relation coincides with the Josephson equation [25], which was introduced in superconductivity for the development of the corresponding effect. From Equation (7), this equation can be written

$$\frac{\partial}{\partial t}\phi(\mathbf{r},t) \;=\; -(\mu(\mathbf{r},t) - \mu_0) \tag{10}$$

We now combine this equation with the continuity equation. First we take the time derivative of Equation (10). Since the chemical potential depends only on density, after linearization of the current term, one finally gets

$$\frac{\partial^2}{\partial t^2}\phi \;-\; \frac{\rho_0}{m}\,(\frac{\partial\mu_0}{\partial\rho})_0\nabla^2\phi \tag{11}$$

In Equation (11) the derivative in front of the Laplacian is calculated in the ground state. Then this equation reduces to the wave equation, with propagation velocity s equal to

$$s = \sqrt{\frac{\rho_0}{m}(\frac{\partial\mu}{\partial\rho})_0} \tag{12}$$

and frequency ω equal to

$$\omega(q) = sq \tag{13}$$

with q the momentum of the wave. These wave modes are just the superfluid phonons. One can see that the frequency is linear in momentum and then vanishes at $q = 0$, as demanded by Goldstone theorem. It is instructive to calculate the mode wave velocity s in simple cases. For a boson liquid the chemical potential can be calculated at the Hartree level, and can be simply written as $\mu = g\rho$, where g is the strength of the s-wave particle-particle interaction. One then gets

$$s = \sqrt{\frac{\rho_0 g}{m}} \tag{14}$$

This expression coincides with the result of the microscopic many-body theory by Bogoliubov [26]. One can see that the mode is stable only if $g > 0$, i.e., for a repulsive interaction. The phonons are clearly supported in this case by the particle-particle interaction.

In case of Fermions, besides the particle interaction the chemical potential is determined by the Pauli principle, which produces an additional repulsion. If we indeed neglect the effect of pairing and other interactions on the Fermi kinetic energy (weak coupling limit), one easily gets the well known result [27]

$$s = v_F/\sqrt{3} \tag{15}$$

where $v_F = k_F/m$ is the Fermi velocity, being k_F the Fermi momentum, related to the number density by $\rho_0 = k_F^3/3\pi^2$. Pairing and other interactions introduce corrections to this expression, as we will discuss within the microscopic approach. The formalism can be generalized to many component superfluids, a typical situation for neutron stars. In this case Equation (11) becomes a system of equations, that are coupled through the mixed derivatives of the different chemical potentials with respect to the densities of the different components, see ref. [16] where the hydrodynamic approach was developed within a different but equivalent formalism. Furthermore one should include entrainment between neutrons and protons, which can be introduced by a non diagonal effective mass.

We have to notice that in the general expression for the wave velocities (12), one can easily recognize the ratio between compressibility and density inside the square root, which shows that superfluid phonons are also compression sound mode. This can be a little surprising, because it looks from Equation (11) that phonons are mainly phase modes. However the continuity equation couples any phase variations to density variations, no matter how small they are.

2.2. *Microscopic Theory*

The phonon degree of freedom within the microscopic many-body theory of fermion liquid is described by the propagator of the density or spin-density operator. In tun, the propagator is just the linear response function of the system to an external probe. For a normal system the "phonons" are the excitations of particle-hole type. They can be described by the Random Phase Approximation (RPA). In this approximation the propagator $\Pi_{ik}(t,t')$ is formally the sum of the diagrams of Figure 1, which can be summed up to an integral equation (in time representation). In a multi-components fermion system one gets a linear system of integral equations, that can be written schematically [4]

$$\Pi_{ik}(t,t') = \Pi^0_{ik}(t,t') + \sum_{jl} \Pi^0_{ij}(t,\overline{t_1})v_{j,l}\Pi_{lk}(\overline{t_1},t') \tag{16}$$

where $i, j, \cdots$ label the different particle-hole components, $v_{j,l}$ is the effective interaction between them and Π^0 is the free response function, which corresponds to the bubbles appearing in Figure 1 The overlined time variable is integrated, while the integration over the coordinates in the second term at the r.h.s is understood. This system, after Fourier transform to energy representation, becomes an algebraic (linear) system of equations, provided the interactions are local. The poles of the response function correspond to the energy of the excitations, and the residues to their strength. Specifically, for the considered Neutron Star matter one has neutron, proton and electron components (neglecting muons), and to each one of them one associate the proper particle-hole operator.

If neutrons and protons are superfluid, one has to enlarge the operators associated to these components. If we take into account both proton and neutron pairing, in terms of creation and annihilation operators the indexes $i, j, \cdots$ must run now over the following configurations

$$
\begin{aligned}
&a^\dagger(p)\,a(p)|\Psi_0> \;\;,\;\; a^\dagger(p)\,a^\dagger(p)|\Psi_0> \;\;,\;\; a(p)\,a(p)|\Psi_0> \\
&a^\dagger(n)\,a(n)|\Psi_0> \;\;,\;\; a^\dagger(n)\,a^\dagger(n)|\Psi_0> \;\;,\;\; a(n)\,a(n)|\Psi_0> \\
&a^\dagger(e)\,a(e)|\Psi_0>
\end{aligned}
\tag{17}
$$

where the labels n, p, e indicate neutrons, protons and electron respectively, and $|\Psi_0>$ is the correlated ground state. If we call A_i the generic configuration, the response functions can be written

$$
\Pi_{ik}(t, t') \;=\; -<\Psi_0|T\{A_i\,(t)A_k^\dagger(t')|\Psi_0> \tag{18}
$$

where T is the usual time ordering operator for bosons, since the configurations of Equation (17) have boson character. The configurations (17) correspond in fact to both density and pairing excitations. One can still consider the sums of diagrams in Figure 1, provided each line can be now represent either a normal or an anomalous single particle propagator, which explicitly reads

$$
G(1,2) \;=\; -\imath<T(\psi(1)\psi^\dagger(2))> \qquad\qquad F(1,2) \;=\; -\imath<T(\psi(1)\psi(2)> \tag{19}
$$

respectively. Here ψ and $\psi^\dagger$ are the fermion destruction and creation operators, and their argument $i = 1, 2$ stand for coordinate, spin and time variables. The free response function $\Pi^{(0)}$ is the the product of two single particle propagators, and Equation (16) still formally holds. In agreement with (17), in principle Equation (16) form a 7×7 system of coupled equations. However, it turns out [7,28] that two equations can be decoupled to a good approximation by taking suitable linear combinations of the pairing additional mode $a^\dagger(p)\,a^\dagger(p)$ and pairing removal mode $a(p)\,a(p)$. In this way the system reduces to 5×5 coupled equations. For later discussion we report here their explicit expression

$$
\begin{pmatrix}
1 - X_+^p U_p & -2X_{GF}^- v_{pp} & 2X_{GF}^- v_c & -2X_{GF}^- v_{pn} & 0 \\
X_{GF}^p U_p & 1 - 2X_p^{ph} v_{pp} & 2X_p^{ph} v_c & -2X_p^{ph} v_{pn} & 0 \\
0 & 2X^e v_c & 1 - 2X^e v_c & 0 & 0 \\
0 & -2X_n^{ph} v_{np} & 0 & 1 - 2X_n^{ph} v_{nn} & X_{GF}^n U_n \\
0 & -2_{GF}^n v_{np} & 0 & -2X_{GF}^n v_{nn} & 1 - X_+^n U_n
\end{pmatrix}
\begin{pmatrix}
\Pi_S^{(p)} \\ \Pi_S^{(ph,p)} \\ \Pi_S^{(ph,e)} \\ \Pi_S^{(ph,n)} \\ \Pi_S^{(n)}
\end{pmatrix}
=
\begin{pmatrix}
\Pi_{0,S}^{(p)} \\ \Pi_{0,S}^{(ph,p)} \\ \Pi_{0,S}^{(ph,e)} \\ \Pi_{0,S}^{(ph,n)} \\ \Pi_{0,S}^{(n)}
\end{pmatrix}
\tag{20}
$$

The definitions of the different terms will be given in the sequel. Details on the equations and their explicit analytic form are given in Appendix A of ref. [29] [1]. The system has to be solved for the response functions Π_{ik}. The indexes i, k run over the configurations of Equation (17) and all of which can be obtained by selecting the inhomogeneous term in Equation (16). More precisely one has to select a given configuration indicated by the right index k and solve the system for each choice of k. In this way one gets all the diagonal and non-diagonal elements of Π_{ik}. The index k is not explicitly indicated in Equation (20), to avoid a too heavy notations, since it is the same at the right hand and left hand sides of the equation and it is running. The left indexes i are displayed according their meaning, as explained below.

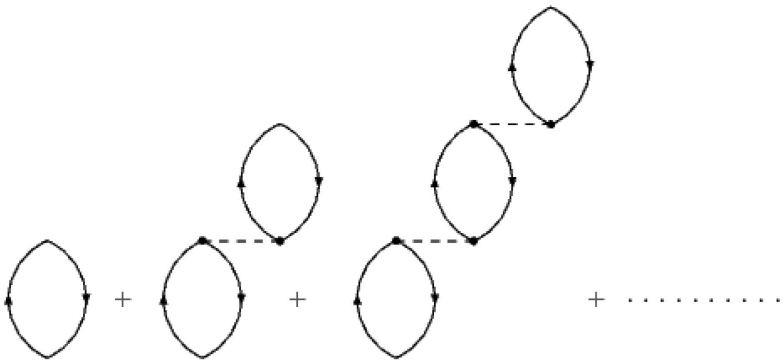

Figure 1. The diagram series of the RPA approximation for the response function of a normal quantum liquid. The bubbles correspond to particle-hole excitations (upward and downward arrows) in the case of a normal system. Backward diagrams are also to be included. For superfluid quantum liquid each line can correspond both to normal and to anomalous propagator.

The effective interaction matrix elements that couple particle-hole configurations to particle-hole configurations can be taken as in the normal system, because the nuclear superfluidity can be considered in the weak coupling regime. The interaction between particle-particle configurations is the same that generates the superfluid pairing. Neutron-proton pairing can be neglected in the neutron tars environment, since neutron and proton Fermi spheres are quite different. Finally no explicit interaction matrix elements between these two types of configurations can appear, if we demand that the interaction conserves the number of particles (weak coupling), but the coupling is produced by those "bubbles", represented by the factors Π^0, which contain a normal and an anomalous single particle propagator, since they indeed do not conserve the number of particles.

The microscopic theory in principle can be applied in the non-linear regime. For instant it can include the pair-breaking mode, where the excited state corresponds to the breaking of a Cooper pair, which occurs at twice the pairing gap. However this excitation is not a "phonon" in the usual sense.

More important is the possibility to calculate the spectral function of the different modes. Let us consider the diagonal matrix element of Equation (18) for a specific component k and its Fourier transform $G_k(E)$. Because $\Pi(t - t')$ depends only on the time difference $\tau = t - t'$, one has ($\hbar = 1$)

$$G_k(E) \;=\; \int d\tau \Pi_{kk}(\tau) \exp(\imath E \tau) \tag{21}$$

Taking into account the time order operator, one gets

$$G_k(E) \;= < \Psi_0 | A_k \frac{1}{E - H + \imath\epsilon} A_k^\dagger | \Psi_0 > - < \Psi_0 | A_k^\dagger \frac{1}{E + H - \imath\epsilon} A_k | \Psi_0 > \tag{22}$$

[1] Notice that the last matrix element at the fifth row and fifth column in the matrix of (20) was misprinted in ref. [29].

where H is the hamiltonian and ϵ is a positive infinitesimal (for convergence). If we now insert the identity in energy representation, one gets

$$G_k(E) = \int dE' | < \Psi_0 | A_k | E' > |^2 \left[\frac{1}{E - E' + \imath\epsilon} - \frac{1}{E + E' - \imath\epsilon} \right] \tag{23}$$

The spectral function $S(E)$can be defined through the imaginary part of $G(E)$ for $E > 0$

$$S_k(E) = -\frac{1}{\pi} Im(G_k(E)) = | < \Psi_0 | A_k | E > |^2 \tag{24}$$

The spectral function is thus the overlap between an eigenstate $|E >$ with a given configuration $A_k|\Psi_0 >$. In particular for an eigenstate of the discrete spectrum there will be no spread of the strength for any component and the spectral function will appear as a sharp peak with zero width (i.e., a delta function). Expression (24) provides a practical way to calculate the spectral function without resorting explicitly to diagonalization.

3. Neutron Pairing

In the inner crust of neutron stars a gas of neutron is present, while at low temperature the protons are still confined inside nuclei. The neutron gas is expected to extend just below the crust in the core, where homogeneous asymmetric nuclear matter appears with a certain fraction of protons. In this region pure neutron pairing should be present in the $^1S_0$ neutron-neutron channel. In the inner crust one should consider the effect of nuclear lattice. This will be discussed in the sequel. Here we treat the neutron gas as homogeneous. Furthermore in the inner core neutron pairing in the $^3P_2$ channel is expected to occur. In this case the phonon structure and spectrum are quite complex, as it will be discussed later.

Let us start with the case of pure neutron pairing, i.e., neglecting all interactions rather than pairing. In this case the pertinent equations are obtained by restricting the system (20) to the last two rows and columns, and putting the particle-hole neutron-neutron interaction v_{nn} to zero. The phonon energy can be identified from the pole of the particle-hole propagator, which, taking into account the explicit expression of Π_0, reads

$$\Pi_S^{ph,n} = 2\left[X_{ph}^n - U_n X_{GF}^n / (1 - X_+^n U_n)\right] \tag{25}$$

where X_{ph} is the neutron (superfluid) free particle-hole propagator, X_+ the particle-particle propagator, X_{GF} the convolution of the mixed product of a normal and an anomalous single particle propagators. Their explicit expressions are reported in the Appendix of ref. [7]. Finally U_n is the effective neutron pairing interaction. All the propagators are functions of the momentum-energy four vector $q = (\mathbf{q}, \omega)$. The pole comes from the zero of the denominator in Equation (25)

$$1 - X_+^n U_n = 0 \tag{26}$$

It turns out that this equation at $q = 0$ coincides with the BCS gap equation, which means that the spectrum $\omega(\mathbf{q})$ of the phonon starts at zero, in agreement with Goldstone theorem, and actually it is linear at small momenta, as it can e verified by expanding the propagator in $|\mathbf{q}|$. The expansion shows that the phonon velocity is the same as in the hydrodynamic treatment, Equation (15), as it must be. This same velocity is recovered for the first sound of normal Fermi liquid [30] in the weak coupling limit. The reason is that the mode also in this case is a pure compressional one, where local equilibrium applies. This is at variance with the superflud phonon, where no collision is present and the compression is induced by the local variation of the order parameter phase. In this sense the phonon is more similar to the zero sound mode of normal Fermi liquid.

If we introduce the neutron particle-hole interaction v_{nn}, the small momentum expansion gives the phonon velocity v_S

$$v_S = \frac{v_F}{\sqrt{3}} \left[1 + F_0 \left(1 - \frac{\Delta^2}{E_F^2}\right)\right]^{\frac{1}{2}} \tag{27}$$

where Δ is the pairing gap and F_0 the $l = 0$ Landau parameter, with the Fermi energy $E_F = \hbar^2 k_F^2/2m = \hbar^2(3\pi^2\rho_0)^{2/3}$. One can see that the effect of pairing on the value of the velocity is small, since Δ/E_F is expected to be quite small, except possibly at very low density. Putting $\Delta = 0$ in (27) one recovers the first sound velocity of normal Fermi liquid [30].

The particle-hole interaction has an additional effect, that is the possibility of decay of the phonons due to Landau damping. This occurs whenever the pole occurs at $\omega > 2\Delta$ and merges into the continuous spectrum of the uncorrelated pair-breaking excitations.

Finally one has to mention that in the crust the neutron superfluid phonon can mix with the lattice phonon, at least for low enough momentum, where the lattice phonons and superfluid phonons can have comparable energies [19,31], with deep consequences on the spectrum and the damping of the excitations.

4. Proton Pairing

Protons are expected to be superfluid, starting from just below the crust in the core, but its extension at even higher density is rather unknown. In addition to the pairing interaction, in this case one needs to include the Coulomb interaction between protons and of protons with the electrons. The pairing itself is of course hindered by the repulsive Coulomb proton-proton interaction. However the electron screening reduces the repulsion and proton pairing is expected to occur. Similar considerations apply to the phonon case. Without screening the superfluid phonon is not possible. In fact the pure Coulomb repulsion is of long range character and it produces plasma excitations, which usually occur at much higher energy than 2Δ, and the excitation spectrum starts at $\mathbf{q} = 0$ mainly at the plasma energy. Indeed Goldstone theorem is not valid for long range interactions, and the energy does not vanishes at zero momentum. The electron screening is quite effective, since electrons are much faster than protons and they can follow the proton oscillations. In other words in first approximation one can use the static screened Coulomb interaction, which is of finite range, at least for not too high momenta. Therefore the proton superfluid phonons are equally possible. The corresponding dynamical equations are obtained by considering the first three rows and three column of the matrix in Equation (20). The meaning of the different terms is the same of the corresponding ones for neutrons. In addition v_c is the unscreened Coulomb interaction and X^e the free electron particle-hole propagator. If we neglect for the moment the proton-proton particle-hole interaction v_{pp} and treat the electron in the static limit, the system is the same as for neutrons, except that we have to add to the pairing interaction the screened Coulomb interaction. Expanding the equations at small momentum, the proton phonon velocity turns out as

$$v_S = \frac{v_F}{\sqrt{3}}\left[1 + \frac{N_p}{N_e}\left(1 - \frac{\Delta^2}{E_F^2}\right)\right] \tag{28}$$

where v_F is now the proton Fermi velocity, and N_p and N_e the density of states of protons and electrons, respectively. Notice that $1/N_e$ is just the screened Coulomb interaction at zero momentum and with the Thomas-Fermi screening length. The correction of the Coulomb interaction turns out to be pretty large, since the proton density of states is much larger than the electron density of states. The velocity v_S can be few times larger than the standard hydrodynamic one [7].

Finally, if the proton particle-hole interaction is introduced, then one has to add to the factor N_p/N_e the proton Landau parameter F_0. Of course also in this case the Landau damping can be active above the pair breaking mode.

5. Neutron-Proton Coupling

The neutron superfluidity in the $^1S_0$ channel is expected to vanish when the NS matter reaches a density close to the saturation one. It is possible that at higher density the proton superfluidity is present, but the neutron superfluidity in the $^3P_2$ channel is weak or absent. Then there will be a region where the proton superfluidity develops in presence of a normal neutron matter. Because of the neutron high density the coupling with the neutron could alter the proton superfluidity. Accordingly, the spectrum of the phonons and their properties will be affected. The pertinent equations are obtained from (20) by suppressing the last row and column. To solve the remaining 4×4 system of equations is a little cumbersome, but numerical solutions are easy to implement. We report some results from ref. [32] to illustrate the salient features of this physics case. The spectral functions of Equation (24) in the particle-hole channel of the three components elucidate quite clearly their coupling and the structure of the phonons spectrum.

In Figure 2 are reported the spectral functions of neutrons (thick black line), protons (thin red line) and electrons (green dashed line) at saturation density of NS matter, with parameters extracted from microscopic calculations [7] and pairing gap $\Delta = 2$ MeV. On the left panel (a) the neutron-proton interaction is present, while on the right panel (b) the interaction is switched off. From the figure one can notice few qualitative features. First of all the neutron spectral function is a broad structure, because the neutron-neutron interaction is attractive and then Landau damping is active. However the neutron-proton interaction affects substantially the neutron spectral function, despite the proton fraction is small, around 4%. Second, the electron spectral function follows closely the proton one, which means that the screening at the indicated momentum is quite effective. Third, the peak in the proton spectral function below 2Δ corresponds to the pseudo-Goldstone mode discussed in Section 4. It should be undamped, i.e., a sharp peak. The finite width is due to the coupling of protons with electrons. The latter at this momentum and energies are Landau damped, which is the reason of the finite width of the proton mode. The coupling with neutrons further increases the width. Finally one can notice a broad structure above 2Δ. This is the proton pair breaking mode, which is over-damped and there is not a definite relation between its energy and its momentum.

The position of the proton peak corresponds approximately to the zero of the real part of the inverse of the proton particle-hole response function. In the hydrodynamic limit the energy so extracted is linear in momentum. As reported in Figure 3, taken from the same reference,this is true also in the microscopic calculation, but deviation from linearity is present at increasing momentum. In the same figure is reported also the effect of the neutron-proton coupling. The deviation from linearity increases as the energy approaches the pair breaking threshold 2Δ. In this region of momenta also the electron screening is reduced, i.e., the electron spectral function does not follow the proton one so closely, as reported in refs. [5,7].

It has to be noticed that the features of the results are unfortunately dependent on the adopted NN force. In particular one can use Skyrme phenomenological forces, and it turns out [7] that different versions of the force can give different results for the pairing gap and the spectral functions. This is not surprising since Skyrme forces are tested at density not larger than the saturation one and for limited value of the matter asymmetry. The microscopic estimate of the different couplings should me more stable with respect to the choice of the theoretical scheme.

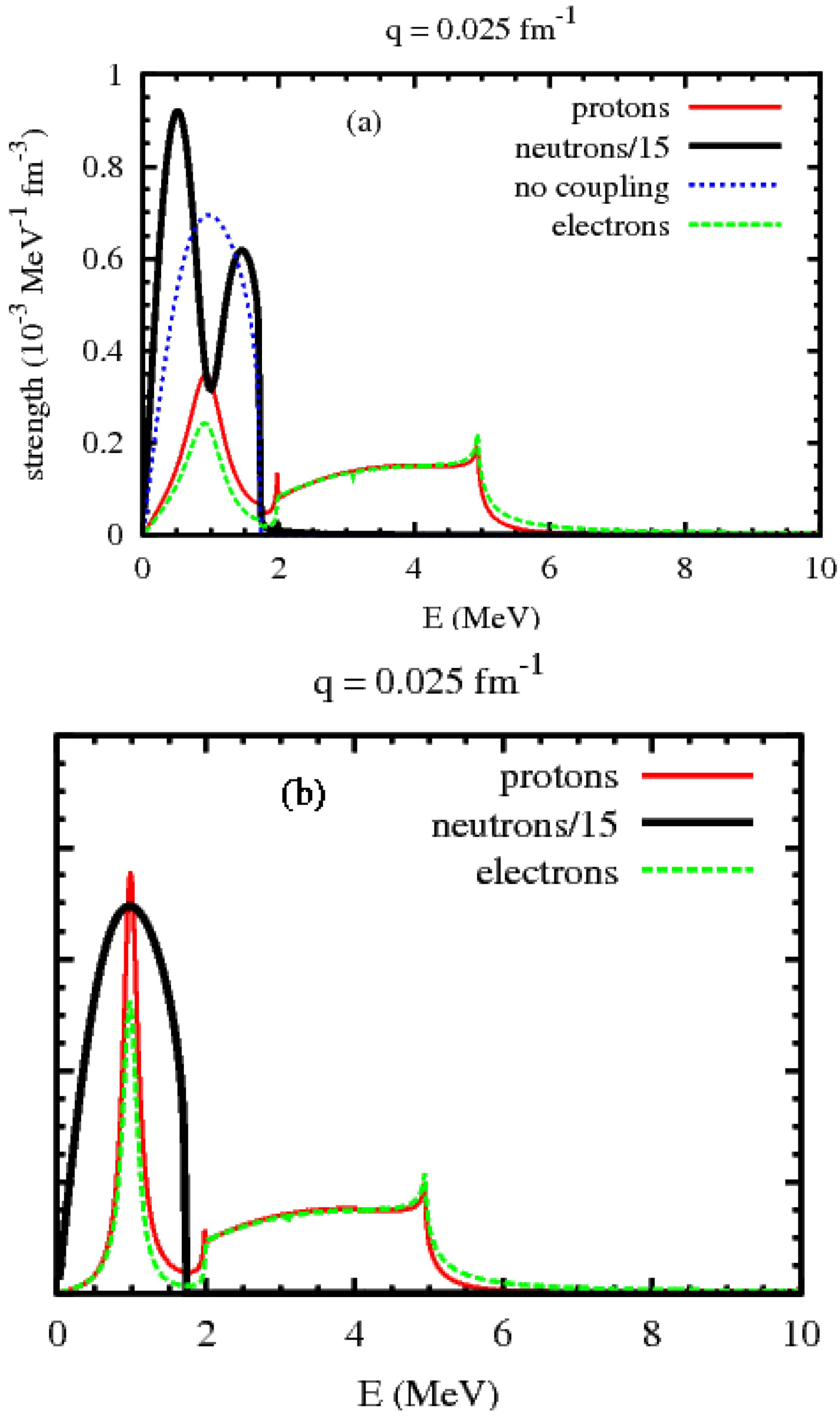

Figure 2. Spectral functions of Equation (24) for neutrons (black thick line), proton (red thin line) and electrons (green dashed line). In panels (**a**) are reported the spectral functions when the Coulomb and nuclear interactions are introduced. For comparison in panel (**b**) are reported the spectral functions when the neutron-proton interaction is neglected. For a closer comparison the neutron spectral function of this case is also reported in panel (**a**) (blue dotted line). Figure form ref. [32].

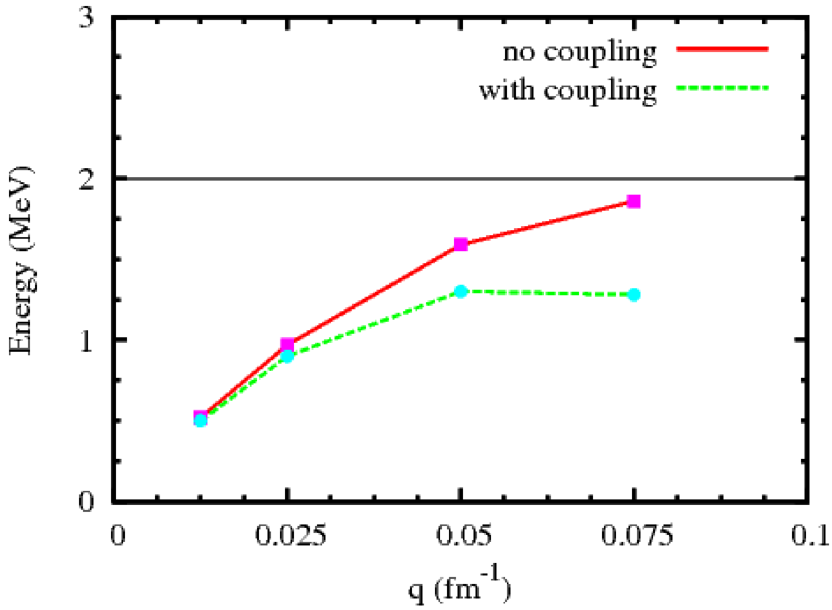

Figure 3. Energy of the zero of the real part of the inverse of the response function at different momenta q. The pairing gap is $\Delta = 1$ MeV. The red full line and full squares correspond to the case when the neutrons and the proton are uncoupled. The green dashed line and the full circles correspond to the case when the interaction between neutrons and protons is switched on. Figure from [32].

6. The Tale of Two Superfluids

The neutron superfluidity in the $^1S_0$ channel is expected to decrease as one proceeds below the crust and should vanish at about saturation density. It is possible that pairing superfluidity is already present at this density. Furthermore at higher density proton superfluidity persists where the $^3P_2 -^3 F_2$ can appear. Therefore there can be regions where neutron and proton superfluidity coexist. In this case the mutual nuclear interaction can modify the pattern of the superfluid strengths, as well as of the phonon spectra and spectral functions of Equation (24). For simplicity we discuss the case where both protons and neutrons are in the superfluid s-wave states.

In this case the full system of Equation (20) has to be used. Notice that despite the absence of the direct interaction between proton pairs and neutron pairs, an indirect (second order) coupling is possible through the anomalous propagator and the neutron-proton particle-hole interaction. Similarly the neutron pairs are coupled with the electrons by the additional proton Coulomb interaction with electrons. The corresponding diagrams are reported in ref. [29].

The neutron, proton and electron spectral functions at a given density and momentum are reported in Figure 4. Also in this case the parameters of the forces are extracted from microscopic calculations. The pairing gaps are taken as typical values expected from theoretical estimates, which unfortunately display a substantial spread. However the qualitative features of the spectral functions should not depend on the their particular values. For neutrons the pairing gap is $\Delta_n = 0.5$ MeV, while for protons the gap is $\Delta_p = 1$ MeV.

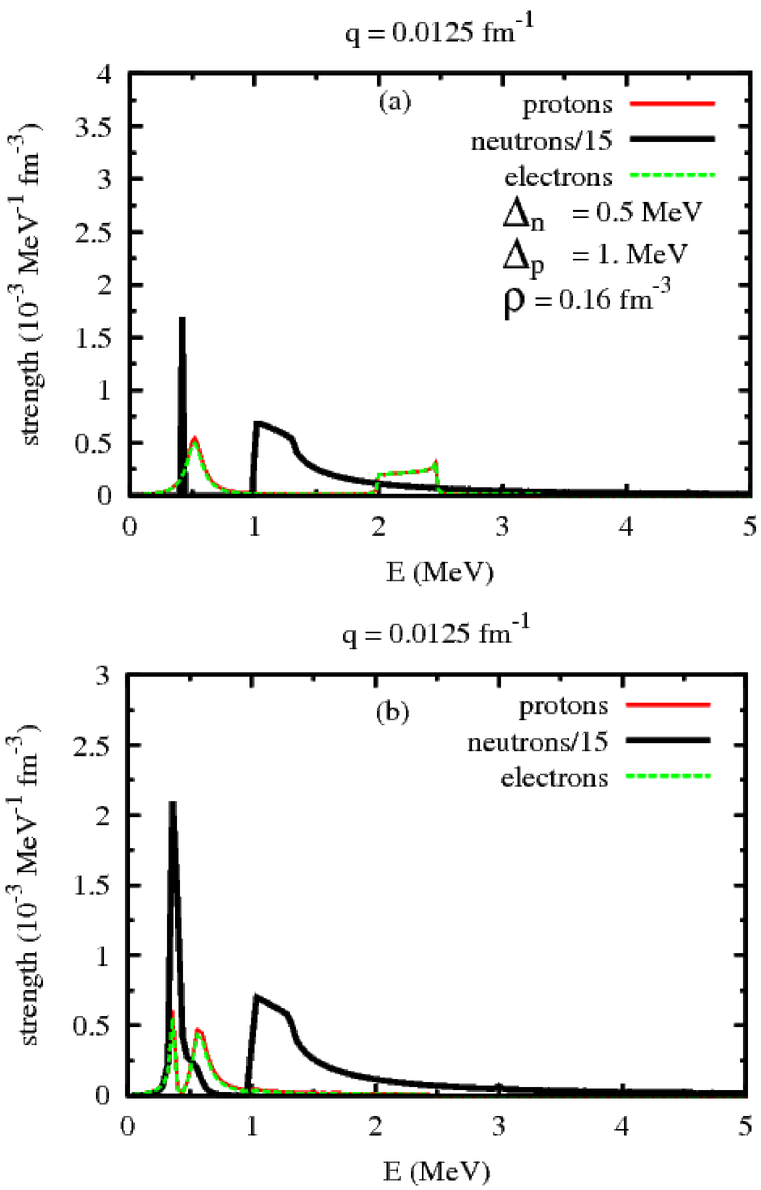

Figure 4. Spectral functions of neutrons (black thick line), proton (red thin line) and electrons (green dashed line) calculated at the total baryon density $\rho = 0.16$ fm^{-3}. The neutron and proton pairing gaps are 0.5 MeV and 1 MeV, respectively. In panel (**a**) the neutron-proton interaction has been suppressed, while in panel (**b**) it is included. For convenience the neutron strength function has been divided by 15. Figure from [29].

In the left panel (a) the neutron-proton coupling is switched off. One notice a neutron sharp peak, corresponding to the Goldstone mode, which is undamped (i.e., a delta function) because it is below $2\Delta_n$ (the height of the peak has no meaning, it is an effect of the plot system). The proton peak below $2\Delta_p$ is also the Goldstone mode, but it is damped by the coupling with the electrons. The latter have a spectral function which follows closely the proton one, since the momentum is small enough. Above twice the pairing gap both neutrons and protons display a trace of the pair breaking mode. When the neutron-proton coupling is switched on, right panel (b), the neutron Golstone mode acquires a finite width by the interaction with protons and indirectly with electrons. In fact, at the position of the peak one can observe the presence also of some strength of the proton and electron spectral functions, while the strength of the pair breaking mode has disappeared.

It can be interesting to see how the pattern of the different phonons changes at higher density and higher momentum. In Figure 5, left panel (a), the results at twice the saturation density are reported, keeping the same values of the pairing gaps and using again the other physical parameters extracted from microscopic calculations. The features of the different spectral functions are similar. The neutron and proton phonons below twice the corresponding pairing gaps are apparent. They have a substantial width, but the corresponding peaks are well pronounced. In addition, some strength of the proton and neutron pair breaking modes still survives.

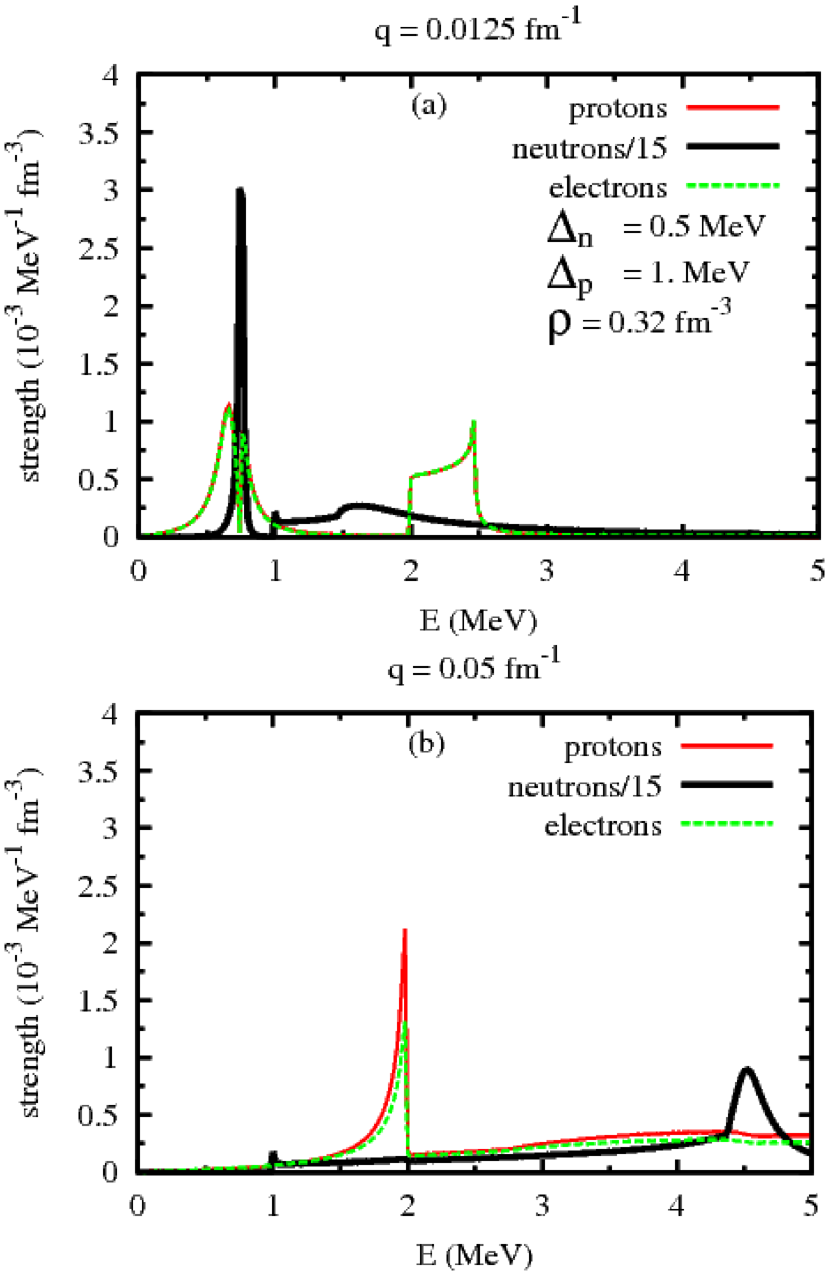

Figure 5. Spectral functions of neutrons (black thick line), proton (red thin line) and electrons (green dashed line) calculated at the total baryon density $\rho = 0.32\ \mathrm{fm}^{-3}$ with the same pairing gaps as in Figure 4, for two different momenta. In both cases the neutron-proton interaction has been included. For convenience the neutron strength function has been divided by 15. Figure from [29].

The situation changes if one considers a higher momentum, right panel (b). The neutron phonon mode has disappeared, while a quite damped peaks appears at higher energy corresponding to the neutron pair breaking mode. It looks that the phonon has moved well above $2\Delta_n$ and became essentially a strongly damped sound mode. The proton phonon still appears evident as an asymmetric peak jut below 2Δ. The electron screening looks only slightly reduced.

From this analysis few conclusions can be drawn. Both neutron and proton superfluid phonons are present in NS matter. In all realistic cases they are damped, so that they have an intrinsic finite mean free path. For small momenta their energy spectrum is linear, but their velocity can be few times different with respect to the weak coupling limit of $v_F/\sqrt{3}$, due to the particle-hole correlations. The superfluid phonons have a natural cut-off at the energy equal to 2Δ, where they merge into the pair-breaking mode, which is essentially a sound mode. If the spectrum remains linear, the momentum cut-off is just $q_c = 2\Delta/v_S$, where v_S is the phonon velocity. However it turns out that deviations from linearity increase as the energy approaches 2Δ, and the momentum cut-off can be substantially different. Furthermore close to the cut-off the damping tends to increase. Proton phonons are present because of the electron screening, which is complete at low momenta, but is weakened at higher momenta, since then the electrons cannot follow the proton dynamics so closely.

Among the features missing in these calculations there is the neutron-proton entrainment, which can be viewed as a non-diagonal effective mass term in the hamiltonian. The entrainment can be traced back to the $l = 1$ Landau parameter F_1, which can indeed include a neutron-proton term. This implies a neutron-proton interaction linear in momentum, which affects the effective mass with a non diagonal contribution. This interaction can be included in the equations (20) as a contribution to v_{pn}. However this needs the introduction, besides the density-density response function, also of the current-density and current-current correlation functions. Then the dimension of the system (20) would increase considerably. The effect of entrainment at microscopic level along these lines has to be yet explored.

7. Superfluid Phonons in Dynamical Processes

The role of phonons in the dynamical processes that can occur in NS has been studied by many authors.

One of the simplest case where the presence of superfluid phonons can be relevant is the specific heat of NS during the cooling process. On one hand the appearance of superfluidity can slow down the cooling evolution because it reduces the rate of neutrino emission, on the other hand superfluidity can accelerate it because of the emission of neutrino [33] or axion [34] from the pair-breaking mode and due to the reduction of the specific heat C_V. The latter effect is related to the energy gap of 2Δ in the excitation spectrum. As a consequence the specific heat below the critical temperature decrease exponentially with the temperature T, namely $C_V \sim \exp(-2\Delta/T)$, which is vanishing small at low temperature. However, at finite temperature the phonon modes can be excited. Overall the phonons behave like a gas of bosons with a spectrum linear in momentum, similarly to the phonons in a crystal lattice or the photons in the black body radiation. Therefore the phonons contribute to the specific heat with a term proportional to T^3. It is clear that such a term must become dominant at low enough temperature. A simple calculations show that this occurs at temperature below to about 100 KeV, then only in the late stage of the cooling.

The presence of a gas of phonons has another consequence. In fact the gas can deviate from an ideal one. Phonon-phonon collisions are possible and, as in ordinary classical gas, this can be a source of dissipation, notably of frictional forces. In particular shear or bulk viscosity is surely present if collisions are not negligible. This affects the dynamical processes in the NS oscillations. Other mechanism of friction are present, in particular electron-electron scattering, nucleon-nucleon scattering or electron-vortex collisions. It is then important to estimate the amount of viscosity due to phonons. To this aim one has to estimate the phpnon-phonon interaction strength. In the hydronynamical regime this can be obtained going beyond the linear approximation, which is equivalent to introduce higher order gradient terms in the wave Equation (11). As we have seen, in the weak coupling limit the strength of the gradient square is determined by the compressibility and therefor by the equation of state of the matter. Higher order terms can then be determined by derivatives of the compressibility with respect to density. From the coupling strength one can then calculate the phonon-phonon scattering rate. All that has been developed in ref. [35,36] for pure neutron matter. Once the scattering probability has been determined, one can describe the evolution of the gas of phonons by means of the Boltzmann kinetic equations [35,36]. In the regime of small deviations from local equilibrium the equation can be solved in a closed form. This provides the modification of the momentum-energy tensor, and from its dissipative part one can extract both shear and bulk viscosity. A detailed comparison with the other dissipation mechanisms seems to indicate the relevance of the role of phonons for the NS oscillation dynamics, in particular the instability of the r-modes [36].

One has however to keep in mind that the phonon spectrum has a cut-off at a certain momentum q_c, determined by the energy cut-off at 2Δ. Therefore all the integrations over the phonon momentum should be restricted up to q_c. It has then to be tested if the introduction of the cut-off affects appreciably all these results.

Thermal conductivity is another process where the superfluid phonons can contribute [37]. In this case it is necessary to calculate the phonon dispersion beyond the linear approximation, because for a linear spectrum the thermal conductivity vanishes, as in the case of a crystal with lattice phonons. The solution of the Boltzmann equations can be used to calculate the heat flux in response to a temperature gradient, and thus the thermal conductivity. In ref. [37] it is claimed that the phonon contribution should be dominant in the core of neutron stars. Also in this case it is unclear the relevance of the necessary cut-off at $\omega = 2\Delta$ of the phonon spectrum.

8. Phonons in the $^3P_2 -^3 F_2$ Neutron Superfluid

In the inner core of neutron stars the superfluidity in p-wave looks possible. In particular in the $^3P_2 -^3 F_2$ channel at increasing relative momentum the neutron-neutron interaction becomes more attractive, as it can be guessed by the behavior of the phase shift. The channel is specified by relative angular momentum $l = 1$, total spin $S = 1$ and total angular momentum $J = 2$. Therefore the structure of the pairing gap can be quite complex, and indeed it has not yet been completely clarified. Recently [38,39] the Ginzburg-Landau theory was used to investigate the possible superfluid phases, corresponding to different gap structure, and it was suggested which one should be the lowest in energy. These results are only partially in agreement with previous works [40,41], and the issue has been not yet clarified.

A peculiarity of the $^3P_2 -^3 F_2$ superfluid phase is the breaking of rotational symmetry, besides the breaking of gauge invariance. This suggests the existence of the corresponding Goldstone modes, in addition to the usual one. These modes are usually called 'angulons'. The pairing gap is in this case a matrix in spin σ and projection M of the total angular momentum. It is expected that the projections M are not equally occupied in the ground state, which corresponds to an alignment of the pairing gap along a symmetry axis. The angulons correspond to oscillations of the pairing gap around the symmetry axis. The existence of angulons was confirmed in ref. [42], where it was shown that the excitation spectrum contains a mode of zero energy at zero momentum. However, according to ref. [43] this mode should acquire a mass as soon as the temperature is finite, even if it vanishes exponentially at zero temperature. This indicates a violation of the Goldstone theorem, since the Goldstone mode should be present for all temperature below the critical one. This must be due to the complex structure of the pairing gap, which clearly contains internal degrees of freedom. These degrees of freedoms are excited at finite temperature. The orientation mode couples to these additional modes, so that the resulting excitation mode is not only a smooth spacial modulation of the orientation of the order parameter, but involves also the internal degrees of freedom. The precise reason of this energy shift, and thus violation of the Goldstone theorem, has still to be completely clarified. Besides the Goldstone mode associated with the breaking of gauge invariance, other modes with a non-zero energy at zero momentum are also present.

In ref. [8] it was pointed out that the coupling of angulons with electrons and between angulons is particularly weak, and therefore their mean free path is quite long, it can be even larger than the size of the star. In general angulons seem not to contribute appreciably to transport phenomena, but they can be efficient in transporting energy due to their long mean free path.

Another process where $^3P_2 - ^3F_2$ angulons can be relevant is the neutrino emission in the NS cooling. In fact the neutrino emission cannot occur from phonons with a linear spectrum in momentum, due to energy-momentum conservation (neglecting neutrino mass). The process is however possible from angulons that are massive, at least at finite temperature. The angulons can in any case acquires mass in a magnetic star, because of the coupling of the neutron magnetic moment with the star magnetic field [44].

All these studies are however neglecting the possible neutron particle-hole excitation, that can couple to the pairing gap excitation. As we have seen in Sections 5 and 6 this coupling can produce a shift in the phonon energy and a possible neutron-neutron Landau damping. In addition a cut-off of the phonon spectrum must be present as soon as the phonon branch crosses the pair-breaking mode, which depends on the structure of the pairing gap, i.e., the particular phase of the superfluid.

9. Concluding Remarks

In this brief review we have presented an introduction to the physics of superfluid phonons in connection with the processes that can occur in neutron stars and their properties. The sketch of the theory discusses and confront the hydrodynamic approach and the microscopic one. As expected, at low momenta the two approaches agree. Besides the deviation from linearity of the phonon spectra at higher momenta, the microscopic approach can include the spectral functions of the different components, which were taken to be neutrons, protons and electrons. The spectral functions can give a vivid view of the coupling between the different matter components and their possible excitations. In particular the electrons are able to screen the repulsive Coulomb proton-proton interaction, and as a result the possible plasma excitation is replaced by a pseudo-Goldstone mode, which turns out to have a much higher velocity than the phonon for a pure superfluid with only pairing interaction. At higher momenta and energy the electron screening is less efficient, that is the electrons are not able to follow closely the proton dynamics. This is clearly apparent in the spectral functions, which are very close at low momenta but less and less close as the momentum increases. Furthermore the electron-proton interaction gives a width to the pseudo-Goldstone mode, which otherwise would be a sharp excitation below 2Δ, the threshold for the pair breaking process. The neutron-proton interaction plays a crucial role in determining the structure of the spectral functions. Besides their distortion the coupling produces an additional width to the proton phonon, particularly if the neutrons are in the Landau damping region for the considered momentum. If also the neutrons are in the superfluid phase, the structure of the excitation spectrum and of the corresponding spectral functions can become more complex. Both neutron and proton pseudo-Goldstone modes are present and they have a finite width. However, if the neutron are outside the Landau damping region, this width is quite small for the neutron spectral function and the excitation looks sharp. This situation seems to be likely at density higher than the saturation one, where the neutron-neutron particle-hole effective interaction is expected to be repulsive. However at higher density it is not expected that both neutrons and protons are both superfluid, at least in the s-wave channel.

At higher density, i.e., in the inner core, the neutrons are expected to be in the p-wave superfluid phase. The particular structure that the pairing gap matrix of the ground state is quite uncertain. This reflects in the difficulty to study the corresponding phonon excitations, which can have several branches due to the internal structure of the gap. However some general characteristic of the possible phonons have been determined. In particular the appearance of "angulons" seems to be well established. These are phonons that correspond to smooth modulations of the orientation of the pairing gap, since the ground state is anisotropic and the Cooper pairs are aligned. They can be considered the Goldsone modes of the superfluid. It seems however that at finite temperature the angulons acquire a mass, i.e., their energy spectrum does not go to zero at zero momentum. This is due to the thermal excitation of the internal degrees of freedoms of the Cooper pairs.

The many phenomena and processes occurring in neutron stars where phonons can play a role have been reviewed and briefly discussed. In general transport processes receive contributions or are affected by superfluid phonons. In some cases it has been argued that they can be dominant. However in these estimate their intrinsic damping, that we have discussed, is neglected, as well as the necessary cut-off in energy at the pair breaking threshold. For these and many other reasons much work has still to be done to estimate accurately the relevance of the superfluid phonons.

Funding: This research received no external funding.

Conflicts of Interest: The author declares no conflicts of interest.

References

1. Sedrakian, A.; Clark, J.W. Superfluidity in nuclear systems and neutron stars. *Eur. Phys. J. A* **2019**, *55*, 167. [CrossRef]
2. Shapiro, S.L.; Teukolsky, S.A. *Black Holes, White Dwarfs and Neutron Stars*; Jhon Wiley and Sons: New York, NY, USA, 1983.
3. Providência, C.; Brito, L.; Santos, A.M.S.; Menezes, D.P.; Avancini, S.S. Coupling of nuclear and electron modes in relativistic stellar matter. *Phys. Rev. C* **2006**, *74*, 045802. [CrossRef]
4. Baldo, M.; Ducoin, C. Elementary excitations in homogeneous neutron star matter. *Phys. Rev. C* **2009**, *79*, 035801. [CrossRef]
5. Baldo, M.; Ducoin, C. Plasmon excitations in homogeneous neutron-star matter. *Phys. At. Nucl.* **2009**, *72*, 1188. [CrossRef]
6. Stetina, S.; Rrapaj, E.; Reddy, S. Photons in dense nuclear matter: Random-phase approximation. *Phys. Rev. C* **2018**, *97*, 045801. [CrossRef]
7. Baldo, M.; Ducoin, C. Elementary excitations in homogeneous superfluid neutron star matter: Role of the proton component. *Phys. Rev. C* **2011**, *84*, 035806. [CrossRef]
8. Bedaque, P.F.; Reddy, S. Goldstone modes in the neutron star core. *Phys. Lett. B* **2014**, *735*, 340. [CrossRef]
9. Kundu, J.; Reddy, S. Neutrino scattering off pair-breaking and collective excitations in superfluid neutron matter and in color-flavor-locked quark matter. *Phys. Rev. C* **2004**, *70*, 055803. [CrossRef]
10. Leinson, L.B.; Perez, A. Vector current conservation and neutrino emission from singlet-paired baryons in neutron stars. *Phys. Lett. B* **2006**, *638*, 114. [CrossRef]
11. Sedrakian, A.; Müther, H.; Schuck, P. Vertex renormalization of weak interactions and Cooper-pair breaking in cooling compact stars. *Phys. Rev. C* **2007**, *76*, 055805. [CrossRef]
12. Leinson, L.B. BCS approximation to the effective vector vertex of superfluid fermions. *Phys. Rev. C* **2008**, *78*, 015502. [CrossRef]
13. Kolomeitsev, E.E.; Voskresensky, D.N. Neutrino emission due to Cooper-pair recombination in neutron stars reexamined. *Phys. Rev. C* **2008**, *77*, 065808. [CrossRef]
14. Yakovlev, D.G.; Kaminker, A.D.; Levenfish, K.P. Neutrino emission due to Cooper pairing of nucleons in cooling neutron stars. *Astron. Astrophys.* **1999**, *343*, 650.
15. Warszawski, A.; Melatos, A.; Berloff, N.G. Unpinning triggers for superfluid vortex avalanches. *Phys. Rev. B* **2012**, *85*, 104503. [CrossRef]
16. Kobyakov, D.; Pethick, C.J.; Reddy, S.; Schwenk, A. Dispersion and decay of collective modes in neutron star cores. *Phys. Rev. C* **2017**, *96*, 025805. [CrossRef]
17. Martin, N.; Urban, M. Collective modes in a superfluid neutron gas within the quasiparticle random-phase approximation. *Phys. Rev. C* **2014**, *90*, 065805. [CrossRef]
18. Martin, N. Modes Collectifs et Hydrodynamiques dans la Croute Interne des Etoiles a Neutrons. Ph.D. Thesis, Université Paris-Saclay, Gif-sur-Yvette, France, 2016.
19. Chamel, N.; Page, D.; Reddy, S. Low-energy collective excitations in the neutron star inner crust. *Phys. Rev. C* **2013**, *87*, 035803. [CrossRef]
20. Martin, N.; Urban, M. Superfluid hydrodynamics in the inner crust of neutron stars. *Phys. Rev. C* **2016**, *94*, 065801. [CrossRef]
21. Kobyakov, D.; Pethick, C.J. Nucleus-nucleus interactions in the inner crust of neutron stars. *Phys. Rev. C* **2016**, *94*, 055806. [CrossRef]
22. Nambu, Y. Quasi-Particles and Gauge Invariance in the Theory of Superconductivity. *Phys. Rev.* **1960**, *117*, 648. [CrossRef]
23. Goldstone, J. Field theories with « Superconductor » solutions. *Nuovo Cimento* **1961**, *19*, 154. [CrossRef]
24. Andersson, N.; Comer, G.L. Relativistic Fluid Dynamics: Physics for Many Different Scales. *Living Rev. Relativ.* **2007**, *10*, 1. [CrossRef] [PubMed]

25. Josephson, B.D. Supercurrents through barriers. *Adv. Phys.* **1965**, *14*, 419. [CrossRef]
26. Fetter, A.L.; Walecka, J.D. *Quantum Theory of Many-Particle Systems*; McGraw-Hill: New York, NY, USA, 1971.
27. Schrieffer, J.R. *Theory of Superconductivity*; W.A. Benjamin, Inc.: New York, NY, USA, 1964.
28. Bardasis, A.; Schrieffer, J.R. Excitons and Plasmons in Superconductors. *Phys. Rev.* **1960**, *121*, 1050. [CrossRef]
29. Baldo, M.; Ducoin, C. Coupling between superfluid neutrons and superfluid protons in the elementary excitations of neutron star matter. *Phys. Rev. C* **2019**, *99*, 025801. [CrossRef]
30. Baym, G.; Pethick, C. *Landau Fermi Liquid Theory*; John Wiley Inc.: New York, NY, USA, 1991.
31. Kobyakov, D.; Pethick, C. Dynamics of the inner crust of neutron stars: Hydrodynamics, elasticity, and collective modes. *Phys. Rev. C* **2013**, *87*, 055803. [CrossRef]
32. Baldo, M.; Ducoin, C. Elementary excitations in homogeneous superfluid neutron star matter: Role of the neutron-proton coupling. *Phys. Rev. C* **2017**, *96*, 025811. [CrossRef]
33. Leinson, L.B. For a recent review. *Adv. High Energy Phys.* **2018**, *2018*, 8963453.
34. Sedrakian, A. Axion cooling of neutron stars. II. Beyond hadronic axions. *Phys. Rev. D* **2019**, *99*, 043011. [CrossRef]
35. Manuel, C.; Tolos, L. Shear viscosity due to phonons in superfluid neutron stars. *Phys. Rev. D* **2011**, *84*, 123007. [CrossRef]
36. Manuel, C.; Tolos, L. Shear viscosity and the r-mode instability window in superfluid neutron stars. *Phys. Rev. D* **2013**, *88*, 043001. [CrossRef]
37. Manuel, C.; Sarkar, S.; Tolos, L. Thermal conductivity due to phonons in the core of superfluid neutron stars. *Phys. Rev. C* **2014**, *90*, 055803. [CrossRef]
38. Mizushima, T.; Masuda, K.; Nitta, M. 3P2 superfluids are topological. *Phys. Rev. B* **2017**, *95*, 140503. [CrossRef]
39. Yasui, S.; Chatterjee, C.; Kobayashi, M.; Nitta, M. Reexamining Ginzburg-Landau theory for neutron 3P2 superfluidity in neutron stars. *Phys. Rev. C* **2019**, *100*, 025204. [CrossRef]
40. Zverev, M.V.; Clark, J.W.; Khodel, V.A. 3P2–3F2 pairing in dense neutron matter: the spectrum of solutions. *Nucl. Phys. A* **2003**, *720*, 20. [CrossRef]
41. Khodel, V.A.; Clark, J.W.; Zverev, M.V. Superfluid Phase Transitions in Dense Neutron Matter. *Phys. Rev. Lett.* **2001**, *87*, 031103. [CrossRef]
42. Bedaque, P.F.; Nicholson, A.N. Low lying modes of triplet-condensed neutron matter and their effective theory. *Phys. Rev. C* **2013**, *87*, 055807. [CrossRef]
43. Leinson, L.B. Collective modes of the order parameter in a triplet superfluid neutron liquid. *Phys. Rev. C* **2012**, *85*, 065502. [CrossRef]
44. Bedaque, P.; Sen, S. Neutrino emissivity from Goldstone boson decay in magnetized neutron matter. *Phys. Rev. C* **2014**, *89*, 035808. [CrossRef]